UHPLC-Q-Orbitrap metabolomics of Syrah red wines during bottle ageing: Molecular markers of evolution and cork permeability

Luca Garcia, Emmanuelle Meudec, Nicolas Sommerer, François Garcia, Cédric Saucier

Food Chemistry 464 (2025) 141517

Contents lists available at ScienceDirect

Food Chemistry

journal homepage: www.elsevier.com/locate/foodchem

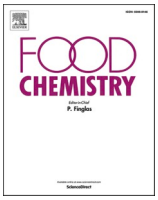

UHPLC-Q-Orbitrap metabolomics of Syrah red wines during bottle ageing: Molecular markers of evolution and cork permeability

Luca Garcia [a], Emmanuelle Meudec [a,b], Nicolas Sommerer [a,b], François Garcia [a], Cédric Saucier [a,*]

[a] SPO, Univ Montpellier, INRAE, Institut Agro, Montpellier, France
[b] INRAE, PROBE Research Infrastructure, PFP Polyphenols Analytical Facility, Montpellier, France

A B S T R A C T

An experiment involving the ageing of Syrah red wine was conducted over a period of 24 months, during which the impact of four different micro-agglomerated corks was examined. An untargeted UHPLC-Q-Orbitrap metabolomics analysis was performed and provided valuable insights into the chemical dynamics of red wine evolution. Forty-three specific discriminating compounds were found for non-aged wines, including various CHO and CHON-types molecules. Thirteen specific discriminating compounds were found for 24-months-aged wines including CHO, CHNOS and CHOS compounds. Among them, sulfonated flavanols and pyranoanthocyanins were identified and emerged as key molecular markers of wine ageing. This metabolomics analysis also enabled us to identify specific chemical markers of cork oxygen transfer rate (OTR) influence. Analysis revealed specific molecules linked to corks with low and high OTR such as anthocyanins and proanthocyanins respectively. This research enhances our comprehension of intricate chemical changes during red wine ageing and underscores the potential impact of cork OTR on wine composition.

1. Introduction

Wine constitutes a complex blend of chemical compounds including proteins, amino acids, carbohydrates, phenolic compounds, volatile elements and inorganic substances (Waterhouse et al., 2016). These components significantly impact wine evolution and quality, particularly during ageing (García-Guzmán et al., 2015). Wine ageing, especially for red wines, stands as a crucial phase in the elaboration of high-quality wines. Over time, wine ageing prompts a multitude of reactions which contribute to the gradual enhancement of the wine sensory attributes (Gambuti et al., 2013; Tao et al., 2014).

Non-volatile compounds of wine, such as polyphenols, exert a pivotal role in its quality. Indeed, polyphenols profoundly influence organoleptic traits such as color, astringency and bitterness (Vidal et al., 2004). Due to their inherent reactivity, polyphenols are ideal substrates for reactions occurring during wine ageing (Oliveira et al., 2011).

The primary transformation that takes place during red wine ageing concerns its color. The intense violet-red hue gradually turns into a reddish-brown brick tint (Ribéreau-Gayon et al., 1998). This can be explained by the evolution of native anthocyanins, as their concentration decrease with time (Alcalde-Eon et al., 2006). These compounds react with other constituents within wine such as flavanols (Salas et al., 2004), yeast metabolites or oxidation compounds like acetaldehyde, pyruvic acid or glyoxal (de Freitas & Mateus, 2011; Fulcrand et al., 1998). Consequently, new pigments are formed that lead to the stabilization of wine color (Echave et al., 2021).

As red wine ages, noticeable alterations occur in mouthfeel attributes, including a decrease of astringency and bitterness. These changes stem from oxidative and non-oxidative polymerizations (Echave et al., 2021) and the precipitation of phenolic compounds like tannins, particularly during bottle ageing. Some authors (Arapitsas et al., 2014) suggest that tannins can interact with sulfur dioxide, leading to flavanol sulfonates. This reaction potentially contributes to the observed reduction in astringency during red wine ageing.

All these changes are influenced by the stopper. Indeed, the ingress of oxygen through the bottle stopper is a significant factor that impacts wine shelf life.

Many studies on the evolution of non-volatile wine compounds use targeted approaches (profiling) (Leborgne et al., 2022; Vrhovsek et al., 2012; Zhang et al., 2021), which consist in the analysis of a predefined group of metabolites. These focused analyses are precise but might overlook a significant portion of the wine molecular information (Alañón et al., 2015). On the other hand, untargeted metabolomics (fingerprinting) emerges as a potent method for capturing the molecular fingerprint of complex beverages like wine (Arbulu et al., 2015; Leborgne et al., 2023).

* Corresponding author.
E-mail address: cedric.saucier@umontpellier.fr (C. Saucier).

https://doi.org/10.1016/j.foodchem.2024.141517
Received 27 October 2023; Received in revised form 26 August 2024; Accepted 30 September 2024
Available online 5 October 2024

Metabolomic methodologies possess the capacity to detect a vast array of molecules and to discern various compounds and distinguish diverse sample types without the necessity of identifying or quantifying each individual compound. These approaches involve a dedicated workflow, i.e. a series of sequential stages, data acquisition, feature extraction, data processing, differential analysis, compound annotation and identification (Utpott et al., 2022). Distinct statistical and visualization tools are employed for conducting differential analysis. Some unsupervised techniques may be used such as principal components analysis (PCA) and hierarchical clustering (Cuadros-Inostroza et al., 2010; Leborgne et al., 2023; Roullier-Gall et al., 2017). Supervised methods like partial least squares-discriminant analysis (PLS-DA) (Arapitsas et al., 2014; Hong, 2011), are often useful and used as well to visually portray patterns within datasets. Furthermore, the application of statistical tests, for example Student's *t*-tests and univariate analysis of variance (ANOVA) show the differences between different groups. To compare two groups, a volcano plot, can be employed. This plot depicts the fold change in signal abundances against the *p*-value of the statistical difference between groups, facilitating the identification of the most discriminant compounds (Baleiras-Couto et al., 2023; Dias et al., 2023). Another objective is then to annotate the compounds. Several approaches are available to achieve this such like comparison of retention times and mass spectra accuracy or the analysis of MS/MS spectra with a standards or with databases or the use of molecular networks (Morehouse et al., 2023).

Recent non-targeted wine analysis studies used analytical techniques like NMR and mass spectrometry. These investigations aimed to discriminate wines according to different factors such as terroir (Gil et al., 2020), varietal characteristics (Delcambre & Saucier, 2013), winemaking influence (Leborgne et al., 2023) and wine age (Arapitsas et al., 2014; Deshaies et al., 2020; Roullier-Gall et al., 2015; Roullier-Gall et al., 2016).

However, to our knowledge, the impact of cork OTR on the evolution of the non-volatile metabolome of red Syrah wines during bottle ageing has never been described. This article is then structured around the following objectives:

- To evaluate the non volatile chemical composition of Syrah red wines during bottle ageing by untargeted metabolomic analysis with ultra-high performance liquid chromatography-high resolution mass spectrometry experiments.
- To discover specific discriminating non volatile compounds linked to cork OTR

The research hypotheses are that known or unknown non volatile compounds may increase or decrease due to wine ageing and the influence of cork OTR.

2. Materials and methods

2.1. Chemicals

LC − MS-grade acetonitrile and formic acid were purchased from Biosolve (Dieuze, France) and purified water was obtained from a Milli-Q water Millipore system (Bedford, MA, USA).

2.2. Wine samples and stoppers

Six samples of red wines, all 100 % Syrah, were collected from various wineries situated in the Côtes du Rhône and Languedoc-Roussillon areas. The summary of wine characteristics (wine name, origin, vintage and ageing method) are outlined in Table 1.

Four distinct microagglomerated cork stoppers (44 ± 0.2 × 24 ± 0.1 mm) were supplied by DIAM Bouchage company based in Céret, France. Oxygen transfer rates (OTR) and initial oxygen rates (OIR) data were measured by a luminescence-based technology and provided by the supplier (refer to Table 1).

Table 1
Characteristics of the red wine samples and corks.

Code	Denomination of origin	Vintage	Ageing
CR1	Côtes du Rhone	2020	Tank
LR1	Languedoc-Roussillon	2019	Oak barrel
LR2	Languedoc-Roussillon	2019	Oak barrel
LR3	Languedoc-Roussillon	2019	Tank
LR4	Languedoc-Roussillon	2019	Oak barrel
CR2	Côtes du Rhone	2019	Oak barrel
Code	**Type**	**OIR (mg)**	**OTR (mg/year)**
DIAM 1 (D1)	Microagglomerate cork	0.77 ± 0.03	0.3 ± 0.1
DIAM 2 (D2)	Microagglomerate cork	1.72 ± 0.25	0.9 ± 0.1
DIAM 3 (D3)	Microagglomerate cork	1.76 ± 0.15	1.1 ± 0.1
DIAM 4 (D4)	Microagglomerate cork	2.19 ± 0.13	1.8 ± 0.4

The bottling of the six wines followed conventional winemaking techniques. Before bottling, levels of free SO_2 were adjusted to 30 mg. L^{-1}. Using a filling machine, 0.75 L empty Bordelaise bottles were manually positioned and nitrogen-inerted. After dispensing 0.75 L of wine into each bottle, cork stoppers manually placed with the aid of a vacuum corker in a random order.

All the biological triplicate combination of bottles and corks were aged during 0 and 24 (t0 and t24) months at 17 °C. At 24 months, 72 bottles were then opened (6 wines × 4 corks × 3 biological replicates).

All combinations of bottles and corks were stored at a temperature of 17 °C. Once the bottle opened, aliquots were prepared in 2 mL plastic vials under argon gas and promptly frozen at −80 °C.

2.3. Enological parameters of wine samples

Classical chemical analyses of wines were carried out for each wine subsequent to bottling at Laboratoires Dubernet (Narbonne, France). The alcoholic percentage was measured through Fourier transformed infrared spectroscopy (FTIR) using the WineScan instrument (FOSS France, Nanterre, France). Total acidity was evaluated employing titration following the OIV-MA-AS313–01 protocol. Volatile acidity, free SO_2 and total SO_2 were quantified using an automated colorimetric method using sequential analyzer. pH was determined utilizing a potentiometric approach. Additionally, iron and copper levels were measured using microwave-induced plasma atomic emission spectrometry (MP-AES) (Agilent France), following to the OIV-OENO 637–2021 guidelines.

2.4. UHPLC-Q-Orbitrap-HRMS

Before injection, wine samples (0 (t0) and 24 months (t24) of ageing) were centrifuged at 10,000 rpm during 10 min, then were diluted 4 times with water. A quality control (QC) sample was prepared consisting in a mix of all the samples of the acquisition sequence (20 µL of each) and will be treated in the same way as the study sample.

These samples were analyzed using a Vanquish UHPLC system manufactured by Thermo Fisher Scientific (Germering, Germany). This system comprised various components, including an autosampler VF-A10-A, a column compartment VH-C10-A, a diode array detector VF-D11-A and a binary pump VF-P10-A. The analytical column employed was a C18 reversed phase Waters Acquity UPLC® HSS-T3 C18 (100 mm × 1.0 mm ID and particle size of 1.8 µm). This column was equipped with an UltraShield UHPLC pre-column filter with a pore size of 0.2 µm, supplied by Restek Corporation (Lisses, France).

0.5 µL of diluted wine sample was injected and the mobile phase was eluted with a consistent flow rate of 0.22 mL.min^{-1}. The chromatographic method was a binary gradient with a mobile phase A (1 % *v*/v aqueous formic acid) and B (80/19/1 v/v/v acetonitrile/water/formic acid). The column temperature was kept at 35 °C. The 24 min elution

process followed a specific gradient: 0–1.5 min at 2 % B, 1.5–4.5 min ramping from 2 % to 12 % B, 4.5–7 min at 12 % B, 7–12 min from 12 % to 24 % B, 12–15 min from 24 % to 48 % B, 15–16 min increasing from 48 % to 60 % B, 16–17 min from 60 % to 100 % B, 17–19 min isocratic at 100 % B, 19–20 min from 100 % to 2 % B, and finally, 20–24 min at 2 % B.

The UHPLC system was hyphenated to an Orbitrap Exploris 480 mass spectrometer from Thermo Fisher Scientific (San José, CA, USA). This mass spectrometer was equipped with an electrospray ionization (ESI) source operating in the positive ion mode. For calibration, an internal post-source fluoranthen mass calibrant (202.0788 *m/z*) was employed. The spray voltage was set to 3500 V, and various gases including sheath gas, auxiliary gas and sweep gas were adjusted to values of 40, 10 and 2 arbitrary units, respectively. Temperatures for the ion transfer tube and vaporizer were set at 280 °C and 300 °C, respectively. The mass range under consideration spanned from m/z 150 to m/z 1500.

The High-Resolution Mass Spectra (HRMS) sample analysis was conducted using the full scan mode, with a resolution set to 240,000. Additionally, a single quality control sample was injected with a higher resolution of 480,000 for identification purposes. MS/MS experiments were carried out with a resolution set to 30,000. The precursor ions were fragmented using High-Energy Collision Dissociation (HCD) against nitrogen gas, with normalized collision energy parameter adjusted to 35 %.

The sample injections followed a specific sequence. It started with three injections of a blank solvent sample, followed by five consecutive injections of a quality control sample. Subsequently, aged or non-aged wine samples were injected in biological triplicate in a randomized manner. After every six wine samples injections, a blank sample and a quality control sample were injected, respectively (Arapitsas & Mattivi, 2018).

2.5. Chemometrics

The HRMS data were processed using 3.2 Compound Discoverer software (Thermo Fisher, Waltham, MA, USA) with a WorkFlow constituted by several steps. The values of the processing parameters of the UHPLC−HRMS data are described in the supplementary material (Table S2). To avoid polar or non-polar contaminating compounds, the features with a retention time (Rt) between 1.5 and 17 min were considered. The data processing resulted in a dataset where the rows corresponded to 842 features, each characterized by a Rt and *m/z* value (Table S0).

First, unsupervised PCA was performed on the dataset using the 3.2 Compound Discoverer software, applying the center and scale options and normalized areas. Then, different volcano plots were used for feature selection. Several comparisons were made: $t = 0$ versus $t = 24$ months for the determination of discriminant compounds of the red wine evolution then D1 cork versus D4 for each wine sample for the determination of the discriminant compounds based on cork oxygen transfer rate differences. The fold change was determined as the ratio of the group 1 / group 2 mean areas, and a log2 transformation was applied to the fold change. Moreover, univariate ANOVA was performed on the same groups and the *p*-values were recorded and a − log10 transformation was applied to the p-values. The volcano plot is the plot of the −log10 p-values versus the log2 fold change for each feature.

2.6. Compounds annotation

First, the elemental formulas of the significant compounds were proposed with 1.7 Freestyle software (Thermo Fisher, Waltham, MA, USA) using the exact mass and the isotopic profile by setting chemical constraints (O/C ratio $\leq$ 1; H/C ratio $\leq$ 4; element counts: C $\leq$ 50, H $\leq$ 100, O $\leq$ 50, $N \leq 20$, S $\leq$ 5) and mass tolerance set at 2 ppm. The calculated elemental formulas were validated by comparison of the mass error difference (in ppm) which is the difference between the theoretical mass and the detected mass. The relative intensities obtained between the experimental and calculated isotopic peaks were also checked. In particular, the isotope-ratio and patterns at ultra-high resolution was used to determine the chemical formula of the studied compounds. Actually, resolved ^{15}N peak vs. ^{13}C peak in the M + 1 experimental isotopic pattern and resolved ^{34}S peak vs. ^{18}O peak and $2x^{13}C$ peak in the M + 2 experimental isotopic pattern were compared to the M + 1 and M + 2 theoretical patterns.

Then, putative compound annotation was performed manually for some compounds by comparing the calculated elemental formula with internal database extracted from previous work of the research group (Dias et al., 2023; Gil et al., 2020; Leborgne et al., 2023) based on relative retention times and MS/MS fragmentation. Online databases were also used such as KEGG (Kyoto Encyclopedia of Genes and Genomes), Phenol-Explorer (http://phenol-explorer.eu/), ChemSpider (https://www.chemspider.com/), PubChem (https://pubchem.ncbi.nlm.nih.gov/).

3. Results and discussion

3.1. Post bottling enological characterisation

The six Syrah red wines were characterized just after bottling and the oenological parameters were given in Table S1.

Volatile acidity content spanned from 0.31 to 0.67 g.L^{-1} H_2SO_4, all falling below the authorized limit of 0.98 g.L-1 H_2SO_4, as stipulated by OIV resolutions. Total acidity fluctuated between 2.72 and 3.41 g.L^{-1} tartaric acid, while pH ranged from 3.64 to 3.97. Furthermore, ethanol percentages ranged between 12.95 % and 16.16 %. These parameters were in line with usual values for red wines originating from the southern regions of France.

Before bottling, free SO_2 levels were adjusted to 30 mg.L^{-1} across all wines. Total SO_2 ranged from 48 to 87 mg.L^{-1}. Copper concentrations were observed within the range of 0.34 to 0.53 mg.L^{-1} whereas iron concentrations ranged from 0.70 to 3.13 mg.L^{-1}. This indicated that there was no potential for copper or iron haze precipitation problem as all levels remained below 1 mg.L^{-1} and 10 mg.L^{-1} respectively.

3.2. Untargeted metabolomics by high resolution mass spectrometry (HRMS)

The exploration of chemical variations between the initial non-aged wine samples and those aged for a period of 24 months was conducted through untargeted metabolomics analysis using UHPLC-Q-Orbitrap-HRMS. To achieve this, all the samples, along with Quality Control (QC) samples outlined in section 2.4, were injected into the system in a randomized step as a single batch. The choice of positive ion mode was made due to its enhanced suitability for the detection of anthocyanin pigments and their derivatives. Subsequently, the collected features were initially treated following the procedure outlined in table S2. The resulting outcome was a dataset consisting of 842 distinctive features, which was then used for subsequent statistical analysis.

3.2.1. Metabolomic analysis of red wine bottle ageing

Unsupervised PCA of the dataset is represented in Fig. 1 A. and resulted in a good separation between the different wine types and ageing times. The first axis (PC1) and the second axis (PC2) accounted for 38.1 % and 15.9 % of the overall variance, respectively, and both contributed significantly to this separation.

The projection of the QC samples (mix of all the batch samples), regularly introduced throughout the sequence, were grouped, and closed at a central location. This served as an indicator of the dataset robustness and repeatability.

Moreover, this PCA analysis revealed distinct separation patterns. Wine samples (Table 1) were separated along the primary principal component showing the diversity and the complexity of the terroir and

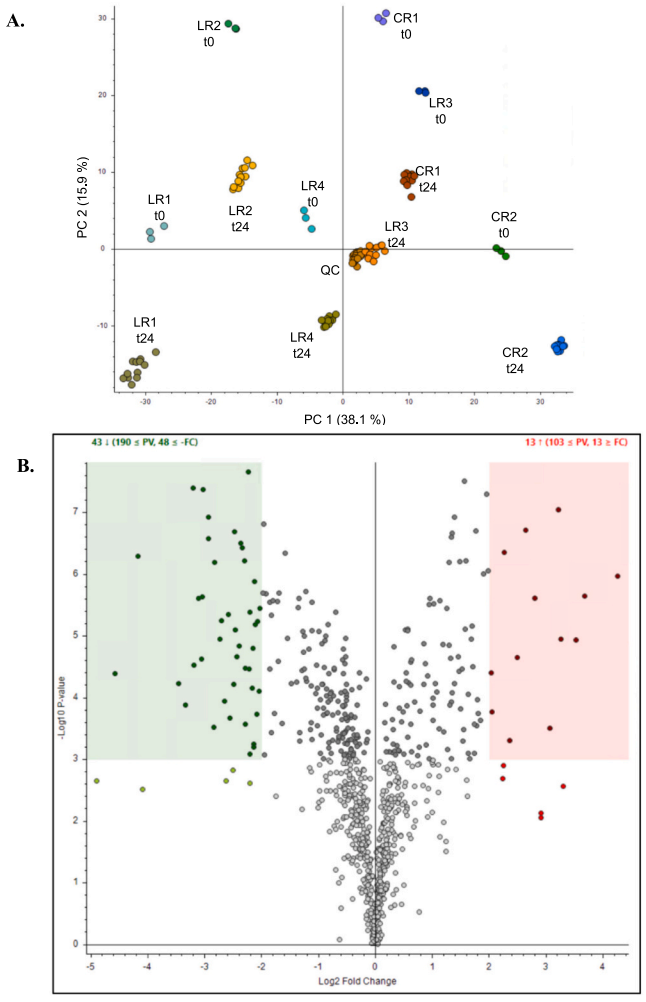

Fig. 1. (A.) Unsupervised PCA analysis from the UHPLC-HRMS features of wine samples (t0 and t24) (explained variance of 54 %). (B.) Volcano plot comparing $t = 0$ month (t0) versus $t = 24$ months (t24). Green and red dots represent discriminating compounds for t0 and t24 wine samples. These compounds are more (green) or less (red) abundant in t0 samples compared to t24 (p-value <0.001; Log2 Fold Change: 2).

the winemaking. Simultaneously, the second principal component contributed to the differentiation between non-aged and aged wines.

Then, with the same dataset, a volcano plot (t = 0 months versus t = 24 months) was generated (Fig. 1B.) to pinpoint the most discriminating features between the two groups (Dias et al., 2023). According to the fold change calculation described in the 2.5. section. Compounds positioned on the left side of the graph (green-shade) were upregulated in t0 samples but downregulated in t24 samples while those located on the right side (red-shade) would imply upregulation in t24 samples, whereas downregulation in t0 samples.

For example, for a value of +2 on the horizontal axis of a given feature, the mean area of t24 wine samples is $2^2 = 4$ times higher than that of t0 samples; and for a value of −2, the mean area of t24 samples is $2^{-2} = 1/4$ of that of t0 samples. Consequently, the green-shaded area encompassed the most discriminating features of t0 samples compared to t24 (43 features, table S3). These features can be considered as markers of evolution of the difference between young and aged wines. A specific molecule might be represented through multiple features sharing identical retention times but exhibiting distinct m/z values. Some of the features were then dereplicated and also tentatively annotated based as described in section 2.6. and 28 features for which a molecular formula could be calculated are shown in Table 2.

These values may correspond for example to molecular or pseudo-molecular ions, adduct and fragment ions, as well as certain isotopic clusters. Actually, although an automatic dereplication of the data was set in the workflow, some features were not properly dereplicated, thus leading to multiple signals for the same compound.

When we looked at the annotated ions discriminating the initial non-aged wines, different types of molecules were identified on the basis of their molecular formula and on literature. Molecules containing nitrogen atoms of the CHON type were identified: Peptides compounds like L-Leucyl-L-Glutamate (260.13713 Da), Glutathione derivative (335.11511 Da) or di-*L*-phenylalanine (312.14733 Da). These compounds may originate from several sources including the grapes or secreted by yeast at the end of fermentation or during their autolysis (Alcaide-Hidalgo et al., 2008; Roullier-Gall et al., 2015). Among the 43 metabolites that exhibited the most significant discrimination of the non-aged wines (t0), the CHO compounds hold paramount importance, especially phenolic compounds. These phenolic compounds encompassed flavonols like isohammetin (316.06561 Da) and glucosides such as quercetin-3-glucoside (464.09566 Da) as well as myricetin-3-O-glucoside (480.09053 Da). These specific flavonols are extracted from grapes during alcoholic fermentation and are present in young wines, then gradually diminish as the wine matures in the bottle (Monagas et al., 2005). A methoxyflavanonol (332.08968 Da) was also identified in this type of metabolites. The only flavanols among the discriminating compounds were an (*epi*)catechin-epigallocatechin dimer (594.13750 Da) and an (epi)gallocatechin dimer (610.13238 Da). These compounds are therefore overexpressed in the initial wines compared to the aged wines because they are more sensitive to oxidation throughout the ageing process as they have the tri-hydroxylated flavonoid pattern. This is also in agreement with previous literature results (Alcalde-Eon et al., 2006; Gambuti et al., 2013). Nine of the identified phenolic compounds were native grape monomeric anthocyanins. These anthocyanins include malvidin-3-O-glucoside (493.13460 Da) along with acetylated derivatives of delphinidin (507.11347 Da), peonidin (505.13406 Da) and malvidin (535.14517 Da). Coumaroylated derivatives of petunidin (625.15573 Da), peonidin (609.16082 Da) and malvidin (639.17138 Da) were also identified. Originating from grapes, these anthocyanins are the main pigments in young red wines. Nonetheless, their abundance diminishes as they undergo various chemical reactions due to their inherent reactivity (Alcalde-Eon et al., 2006; Salas et al., 2004). Certain derived pigments stemming from these reactions may exist in young wines, formed during alcoholic fermentation through interactions with yeast derivatives such as acetaldehyde. These derived pigments might serve as early ageing markers as their concentration increase during the initial months of ageing before further reactions or degradation. This is corroborated by the identification of three isomers of (epi)catchine-ethyl-malvidine-3-O-glucoside (809.22929 Da) among the discriminating metabolites present in the initial wines (Mateus et al., 2002).

Among the ions that discriminate 24-months-old wines from t0 wines (13 features, Table S5) in the red-shaded area (Fig. 1B.),12 features could generate a possible molecular formula (Table 3). Similar to the initial time point (t0), these metabolites corresponded to low molar mass CHON-type compounds (< 300 Da). These particular compounds could be amino acids, peptides or products stemming from the degradation of other peptides or proteins. Peptides and their derivatives mays undergo hydrolysis, oxidation and precipitation during the maturation of wine (Roullier-Gall et al., 2015). Among these CHON compounds, we tentatively identified a compound characterized by the molecular formula $C_{15}H_{20}O_2N_2$ and a mass of 260.15233 Da, which can be tentatively annoted to cyclo(L-Phe-L-Leu).

We also found the emergence of distinctive CHONS-type compounds, such as $C_8H_9O_4NS$ (215.02521 Da), which was previously identified as an antioxidant compound in wine (Romanet, 2019), and $C_9H_{11}O_6NS$ (261.03058 Da). These compounds originate predominantly from sulfonation reactions involving amino acids and peptides (Nikolantonaki et al., 2022). Previous study demonstrated a progressive increase in the

Table 2
Highly discriminating compounds for t0 wines compared to t24 wines tentatively annotated by UHPLC−ESI − Q − Orbitrap MS analyses, Glc = Glucoside, * composition based on exact mass, sequence not determined, mean, median, minimun and maximun area in Table S4.A.

Annotation	RT (min)	Molecular formula	Neutral calculated mass (Da)	Measured m/z	Error (ppm)	Type of compound	Subclass	Log2 (Fold Change)	Log10 (p-value)
Pro-Thr-Lys*	1.602	$C_{15}H_{28}O_5N_4$	344.20607	345.21341	0.29	N compound	peptide	−210,489	517,441
Unknown	2.61	$C_{11}H_{18}O_4N_2$	242.12658	243.13385	−0.34	N compound	peptide	−219,795	538,011
Leu-Glu	2.623	$C_{11}H_{20}O_5N_2$	260.13713	261.14438	−0.34	N compound	peptide	−203,277	410,486
Glutathione derivative	2.649	$C_{12}H_{21}O_6N_3S$	335.11511	336.12256	0.34	N compound	peptide	−292,098	692,236
Alpha-Asp-Phe*	4.441	$C_{13}H_{16}O_5N_2$	280.10583	281.1131	−0.32	N compound	peptide	−242,908	465,854
Glu-Leu-Pro*	5.462	$C_{16}H_{27}O_6N_3$	357.19012	358.19739	0.37	N compound	peptide	−264,612	393,347
methoxyflavanonol	6.76	$C_{17}H_{16}O_7$	332.08968	333.09695	0.24	Polyphenol	flavanonol	−272,248	494,259
Myricetin−3-O-glc	10.888	$C_{21}H_{20}O_{13}$	480.09053	481.09781	0.30	Polyphenol	flavonol	-303,885	563,141
Malvidin-3-O-glc	11.283	$C_{23}H_{25}O_{12}$ +	493.13460	493.13406	−0.54	Polyphenol	anthocyanin	−201,844	544,683
Phe-Phe	11.663	$C_{18}H_{20}O_3N_2$	312.14733	313.1546	−0.21	N compound	peptide	−21,971	308,683
Delphinidin 3-O-(6″-acetyl)glc	12.198	$C_{23}H_{23}O_{13}$ +	507.11347	507.11334	−0.25	Polyphenol	anthocyanin	−222,063	765,566
Quercetin 3-Glucoside	12.572	$C_{21}H_{20}O_{12}$	464.09566	465.10287	0.39	Polyphenol	flavonol	−283,684	351,229
Unknown	12.859	$C_{39}H_{38}O_{18}$	794.20635	795.21362	0.67			−310,794	560,608
Kaempferol 3-*O*-acetyl-glucoside	13.014	$C_{23}H_{22}O_{12}$	490.1112	491.11844	0.16	Polyphenol	flavonol	−227,851	355,997
(Epi)catechin-methylmethine malvidin-3-glc (isomer 1)	13.58	$C_{40}H_{41}O_{18}$ +	809.22929	809.22913	−0.19	Polyphenol	anthocyanin-ethyl-flavanol	−254,942	366,761
(Epi)catechin-methylmethine malvidin-3-glc isomer 2)	13.913	$C_{40}H_{41}O_{18}$ +	809.22929	809.22913	−0.19	Polyphenol	anthocyanin-ethyl-flavanol	−238,729	483,796
Hispidulin	14.166	$C_{16}H_{12}O_6$	300.06326	301.07053	−0.41	Polyphenol	flavone	−212,768	324,032
Peonidin 3-O-(6″-acetyl)glc	14.172	$C_{24}H_{25}O_{12}$ +	505.13406	505.13409	0.06	Polyphenol	anthocyanin	−207,853	373,026
(Epi)catechin-methylmethine malvidin−3-glc (isomer 3)	14.186	$C_{40}H_{41}O_{18}$ +	809.22929	809.22937	0.10	Polyphenol	anthocyanin-ethyl-flavanol	-345,745	421,935
Isorhamnetin	14.223	$C_{16}H_{12}O_7$	316.05834	317.06561	0.13	Polyphenol	flavonol	−457,655	438,288
Malvidin-3-(6‴-acetyl)glc	14.382	$C_{25}H_{27}O_{13}$ +	535.14517	535.14496	−0.39	Polyphenol	anthocyanin	−213,323	319,864
(epi)gallocatechin dimer	14.466	$C_{30}H_{26}O_{14}$	610.13238	611.13971	0.20	Polyphenol	flavanol	−235,532	649,394
Malvidin-3-(6‴-Caffeoyl)glc	14.871	$C_{32}H_{31}O_{15}$ +	655.16630	655.16595	−0.53	Polyphenol	anthocyanin	−292,644	657,624
Epi(cat)-epigallo dimer	14.884	$C_{30}H_{26}O_{13}$	594.1375	595.14484	0.27	Polyphenol	flavanol	−228,502	447,463
Anthraquinone glycoside derivative	14.982	$C_{42}H_{42}O_{19}$	850.23229	851.2395	0.31	Anthraquinone		−318,582	451,756
Petudin-3-(6″-p-coumaroyl)glc	14.998	$C_{31}H_{29}O_{14}$ +	625.15573	625.15533	−0.63	Polyphenol	anthocyanin	−23,348	642,828
Peonidin-3-(6″-p-coumaroyl) glc (cis)	15.068	$C_{31}H_{29}O_{13}$ +	609.16082	609.16052	−0.49	Polyphenol	anthocyanin	−216,445	415,436
Peonidin-3-(6″-p-coumaroyl) glc (trans)	15.321	$C_{31}H_{29}O_{13}$ +	609.16082	609.16058	−0.39	Polyphenol	anthocyanin	−247,773	421,332
Malvidin-3-(6″-p-coumaroyl) glc	15.372	$C_{32}H_{31}O_{14}$ +	639.17138	639.17126	−0.18	Polyphenol	anthocyanin	−228,914	621,556

quantity of CHONS during ageing (Roullier-Gall et al., 2015, Roullier-Gall et al., 2016).

Furthermore, the CHOS compounds were also important for the discrimination of aged wines as they increase during the wine ageing process. These findings are in agreement with the literature (Arapitsas et al., 2014; Nikolantonaki et al., 2022; Roullier-Gall et al., 2017). Sulfonation reactions take place under acidic wine conditions during bottle ageing. In enological conditions, characterized by pH levels between 3 and 4, sulfites are in the form of hydrogenosulfite ions (HSO_3^-), which are susceptible to react with nucleophiles present in wine, especially polyphenols (Arapitsas et al., 2014; Nikolantonaki et al., 2022). (Epi)-catechin-(*epi*)-catechin-SO_3H dimer (658.09964 Da) was tentatively identified as distinctive of red wine ageing markers.

Finally, compounds with a molecular formula composed of CHO constituents exert a notable influence on the evolution of organoleptic attributes of the red wine. Indeed, CHO compounds constitute the primary substrates guiding this evolution, particularly in the context of oxidation reactions. Among these CHO compounds, polyphenols take a predominant place in red wine samples, reacting with numerous compounds during red wine ageing (Echave et al., 2021). Our analyses led to the tentative identification of vitisin A and B (561.12443 Da and 517.13460 Da respectively) as well as pinotin A (at 625.15573 Da). These three pyranoanthocyanins are the result of reactions between malvidin-3-O-glucoside, pyruvic acid, acetaldehyde and caffeic acid (de Freitas & Mateus, 2011). These compounds are red wine ageing markers as they contribute to the brick color of aged wines (Ribéreau-Gayon et al., 1998).

3.3. Metabolomic analysis of the cork OTR influence

Many types of compounds (CHO, CHON, CHONS) can be considered as non-targeted markers of the overall evolution of red wines and can

Table 3
Highly discriminating compounds for t24 wines compared to t0 wines annotated from databases by UHPLC−ESI − Q − Orbitrap MS analyse, mean, median, minimun and maximun area in Table S4.B.

Annotation	RT (min)	Molecular formula	Neutral calculated mass (Da)	Measured m/z	Error (ppm)	Type of compound	Subclass	Log2 (Fold change)	Log10 (p-value)
(Epi)-cat-(epi)-cat Sulfonate	1.853	$C_{30}H_{26}O_{15}S$ $C_{10}H_{12}O_6N_2$	658.09964	659.10693	0.45	Polyphenol	flavanols sulfonate	204,046	439,421
Unknown	1.915	S	288.04161	289.0488	−0.28	N compound		326,582	494,591
Unknown	2.618	$C_9H_{11}O_6NS$	261.03071	262.03781	−0.66	N compound		249,519	464,375
Unknown	2.627	$C_8H_9O_4NS$	215.02521	216.03252	0.12	N compound		265,457	671,012
Unknown	3.287	$C_{12}H_{23}O_2N_3$ $C_{11}H_{14}O_7N_2$	241.17894	242.1862	−0.6	N compound		227,005	634,626
Unknown	5.063	S	318.05216	319.05939	−0.18	N compound		368,974	563,621
Unknown	5.636	$C_{11}H_{11}O_3N_3$	233.07997	234.08725	−0.55	N compound		427,019	596,143
Unknown	6.495	$C_{10}H_{15}O_3N$	197.10515	198.11243	0.32	N compound		301,071	321,071
Vitisin A	12.089	$C_{26}H_{25}O_{14}+$	561.12443	561.12402	−0.73	Polyphenol	pyranoanthocyanin	240,891	321,679
Vitisin B	12.478	$C_{25}H_{25}O_{12}+$	517.13460	517.13416	−0.85	Polyphenol	pyranoanthocyanin	361,382	495,621
Cyclo(Phe-Leu)	15.019	$C_{15}H_{20}O_2N_2$	260.15233	261.15964	−0.57	N compound	peptide	206,073	37,674
Pinotin A	15.416	$C_{31}H_{29}O_{14}+$	625.15573	625.15546	−0.43	Polyphenol	pyranoanthocyanin	331,659	700,231

statistically discriminate between young and aged wines. Nevertheless, it is interesting to consider the potential impact of microagglomerated cork on these non-targeted markers, especially as most cork-related changes are attributed to oxidative mechanisms. Because of its physical properties, the cork will bring oxygen to the wine throughout the ageing of the bottle and this oxygen transfer rate (OTR) and may be a crucial parameter that influences the shelf life of the wine.

When the unsupervised PCA of the data set for the t24 samples was plotted (Fig. 2 A.), the first axis (PC1) and the second axis (PC2) accounted for 42.7 % and 16.3 % of the overall variance respectively.

Nevertheless, when the groups clustered within each wine sample were examined, there was minimal distinction among the various microagglomerated cork stoppers. As a result, the diversity due to the origin of the wine is higher compared to the one of the cork type. Consequently, a basic unsupervised PCA was unable to discriminate the aged samples within the same wine origin.

We therefore generated the volcano plot between the corks which have the most different OTR (D1 versus D4). This volcano plot allowed the determination of the most discriminating features in the two groups representing the compounds over-expressed in the wines corked with the D1 cork (green-shade) and those corked with the D4 cork (red-shade) for all wines (Fig. 2B.). Consequently, the green-shaded area encompassed the most discriminating features D1 wine samples (2 metabolites) while the red-shaded area encompassed the most discriminating features to D4 wine samples (4 metabolites).

The low number of discriminating features between the two groups was consistent with the observations made on the PCA (Fig. 2 A.) where the differentiation associated with the impact of the cork is less pronounced compared to the effect of ageing time or wine origin.

However, these features can be considered as markers of the influence of the cork OTR on red wine ageing as they were very significantly different (p value <0.01) and increased or decreased more than 2^1 folds i.e. 100 % of their initial values. All the features were tentatively annotated based as described in section 2.6. and were shown in Table 4.

Interestingly, after identifying the markers for these two groups, all were CHO-type molecules and more specifically phenolic compounds. This could be explained by the fact that the OTR will influence the oxygen supply to the wine and therefore influence oxidation, polyphenols remaining the main substrates for oxidation reactions (Oliveira et al., 2011). When we looked at the two markers that discriminate cork D1, the cork with the lowest OTR against D4, we saw that they were tentatively annotated as malvidin-3-O-glucoside (493.13460 Da) and malvidin-3-(6″-p-coumaroyl)glucoside (639.17138 Da). These markers were therefore over-expressed in wines corked with cork D1 compared to those corked with cork D4. These results were in agreement with the literature (Gambuti et al., 2013). Indeed, increasing OTR favours the

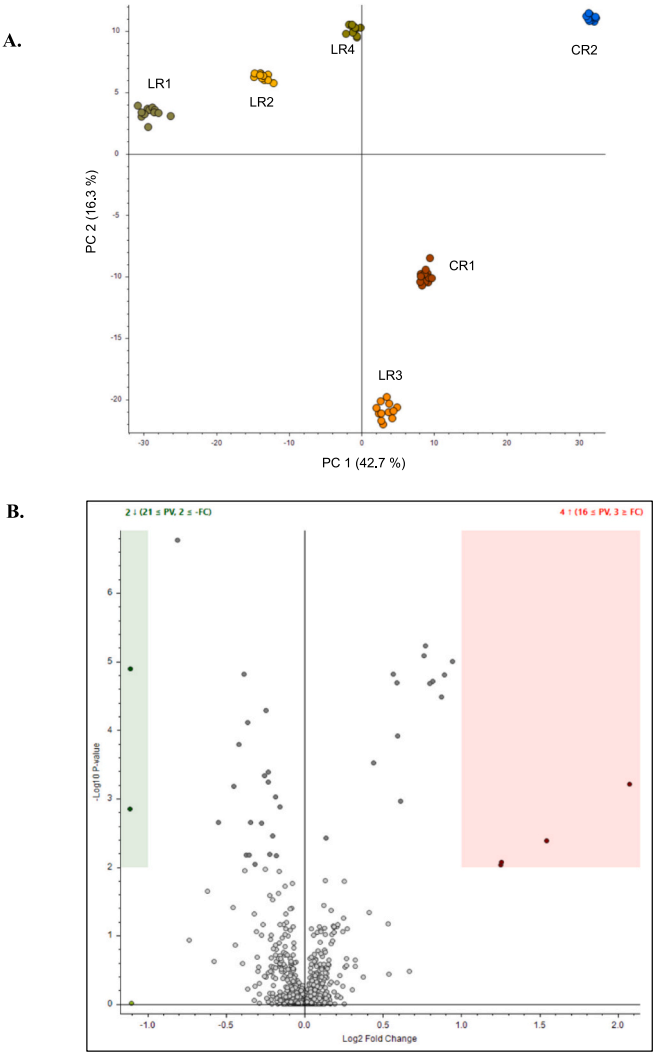

Fig. 2. (A.) Unsupervised PCA analysis from the UHPLC-HRMS features of wine samples after 24 months of ageing (t24) (explained variance of 59 %). (B.) Volcano plot comparing D1 (green) versus D4 (red) at $t = 24$ months. Green and red dots represent discriminating compounds at t = 24 months of D1 and D4 wine samples respectively. (p-value <0.01; Log2 Fold Change: 1).

Table 4
Highly discriminating compounds for D1 and D4 after 24 months of ageing tentatively annotated by UHPLC−ESI − Q − Orbitrap MS analyses. Glc = Glucoside, mean, median, minimun and maximun area in Table S4.C.

Cork	Annotation	RT (min)	Molecular formula	Neutral calculated mass (Da)	Measured m/z	Error (ppm)	Type of compound	Subclass	Log2 (Fold Change)	Log10 (p-value)
D1	Malvidin-3-O-glc	11,283	$C_{23}H_{25}O_{12}^{+}$	493,1346	493,13,406	−0,54	Polyphenol	anthocyanin	−108,749	49,171
	Malvidin-3-(6″-p-coumaroyl)glc	15,372	$C_{32}H_{31}O_{14}^{+}$	639,17,138	639,17,126	−0,18	Polyphenol	anthocyanin	−111,053	284,552
	Caffeic acid	5,98	$C_9H_8O_4$	180,04229	181,04958	0,39	Polyphenol	phenolic acid	125,495	207,507
D4	Vitisin B	12,478	$C_{25}H_{25}O_{12}^{+}$	517,1346	517,13,416	−0,85	Polyphenol	pyranoanthocyanin	156,741	23,541
	Pinotin A	15,416	$C_{31}H_{29}O_{14}^{+}$	625,15,573	625,15,546	−0,43	Polyphenol	pyranoanthocyanin	207,393	320,964

involvement of these molecules in oxygen-activated reactions between anthocyanins to form pyranoanthocyanins and ethyl-bound pigments or favours the chemical degradation of these anthocyanins (Echave et al., 2021; Lopes et al., 2007).

Moreover, when we looked at markers that discriminate wines corked with the cork D4 (highest OTR) against D1 (lowest OTR), caffeic acid (180.04229 Da) was tentatively annotated. This result is surprising since an increase in OTR would lead to an increase in oxidation. However, it has been shown in the literature that an increase in caffeic acid concentration is possible during ageing (Ferreira-Lima et al., 2013; Ginjom et al., 2011; Rihak et al., 2022). This can be explained by hydrolysis of the esterified form, caftaric acid, and this chemical or enzymatical hydrolysis. This link with the oxidation of the medium remained to be confirmed. In addition, pinotin A resulting from the reaction between caffeic acid and malvidin-3-O-glucoside was identified (625.15573 Da) as one of the discriminating markers of the D4 stopper. The concentration of pinotin A is generally higher when caffeic acid concentration is also important (Schwarz et al., 2004). A final oxidation step is also necessary for the re-aromatisation of pinotin A. An increase in OTR would then favour the formation of this compound during bottle ageing. Another pyranoanthocyanin, vitisin B, was tentatively identified (517.13460 Da) as markers of high cork OTR. Indeed, an increased oxygen transfer rate (OTR) results in a greater transfer of oxygen to the wine, which in turn promotes the oxidative conversion of anthocyanins into pyranoanthocyanins, principally through the generation of acetaldehyde. This leads to a consistent rise in pyranoanthocyanins concentration during the initial phase of ageing. The oxygen-rich environment created by the highest OTR conditions encourages the transformation of anthocyanins into alternative resistant pigments that exhibit a more orange tint (de Freitas & Mateus, 2011).

This metabolomic analysis allowed us to identify chemical compounds as potential markers of cork OTR. Oxygen transfer rate from cork is thus a crucial factor impacting wine shelf life. Unsupervised PCA analysis showed limited differentiation among various cork stoppers, emphasizing wines inherent diversity. A volcano plot comparing high and low OTR corks revealed discriminating markers. These markers are primarily CHO-type molecules, and more particularly polyphenols which act as key substrates for oxidation reactions. Low OTR corked wines showed over-expressed malvidin-3-O-glucoside and malvidin-3-(6″-p-coumaroyl)glucoside whereas for high OTR wines there were caffeic acid and pyranoanthocyanins, illustrating the complex OTR effects on wine composition.

4. Conclusion

An untargeted UHPLC-Q-Orbitrap metabolomics analysis provided valuable insights into the chemical dynamics of red wine evolution over a 24-months ageing period. Unsupervised PCA successfully distinguished molecular ions between different wine types and ageing times. Specific compounds discriminated between non-aged and 24-months-aged wines, including various CHO and CHON-types molecules in non-aged wines. An increase in CHO, CHONS and CHOS compounds with ageing time was also evidenced, especially a sulfonated compound. Notably, CHO compounds, particularly polyphenols, emerged as key molecules in wine ageing and especially pyranoanthocyanins, serving as potential evolution markers.

Our metabolomics analysis also shed light on the potential role of specific chemical markers for the influence of cork oxygen transfer rate (OTR) on wine ageing. Unsupervised PCA analysis demonstrated the inherent diversity of wines under various cork stoppers after 24 months of ageing, but a statistical analysis revealed distinct markers associated with low and high OTR corks such as anthocyanins and pyranoanthocyanins respectively.

In conclusion, this study contributes to a better understanding of the complex chemical transformations that occur during red wine ageing and highlights the potential influence of cork OTR on wine composition. Further research in this area could involve the development of targeted LC-MS/MS analysis of some ageing markers found in this study to study their quantitative evolution kinetics during red wine ageing.

Funding

This work was supported in part by a research contract between Diam Bouchage and the University of Montpellier (200893).

CRediT authorship contribution statement

Luca Garcia: Writing – review & editing, Writing – original draft, Methodology, Investigation, Data curation. **Emmanuelle Meudec:** Writing – review & editing, Methodology, Formal analysis. **Nicolas Sommerer:** Writing – review & editing, Methodology, Formal analysis. **François Garcia:** Writing – review & editing, Validation. **Cédric Saucier:** Writing – review & editing, Supervision, Project administration, Funding acquisition, Conceptualization.

Declaration of competing interest

The authors declare that they have no known competing financial interests or personal relationships that could have appeared to influence the work reported in this paper.

Data availability

Data will be made available on request.

Acknowledgements

We acknowledged Diam bouchage company for funding this project and PhD grant of Luca Garcia. Winemakers from Languedoc-Roussillon and Côtes-du-Rhône are thanked for allowing sampling in their cellars.

Vivelys company is acknowledged for its help in wine bottling. We acknowledged also Dr. Aecio L. De Sousa Dias for helpful discussion on volcano plot statistical analysis.

Appendix A. Supplementary data

Supplementary data to this article can be found online at https://doi.org/10.1016/j.foodchem.2024.141517.

References

Alañón, M. E., Pérez-Coello, M. S., & Marina, M. L. (2015). Wine science in the metabolomics era. *TrAC Trends in Analytical Chemistry, 74*, 1–20. https://doi.org/10.1016/j.trac.2015.05.006

Alcaide-Hidalgo, J. M., Moreno-Arribas, M. V., Polo, M. C., & Pueyo, E. (2008). Partial characterization of peptides from red wines. Changes during malolactic fermentation and ageing with lees. *Food Chemistry, 107*(2), 622–630. https://doi.org/10.1016/j.foodchem.2007.08.054

Alcalde-Eon, C., Escribano-Bailón, M. T., Santos-Buelga, C., & Rivas-Gonzalo, J. C. (2006). Changes in the detailed pigment composition of red wine during maturity and ageing : A comprehensive study. *Analytica Chimica Acta, 563*(1), 238–254. https://doi.org/10.1016/j.aca.2005.11.028

Arapitsas, P., & Mattivi, F. (2018). LC-MS untargeted protocol for the analysis of wine. In G. A. Theodoridis, H. G. Gika, & I. D. Wilson (Éds.), Metabolic profiling : Methods and protocols (p. 225–235). Springer. Doi: https://doi.org/10.1007/978-1-4939-7643-0_16.

Arapitsas, P., Speri, G., Angeli, A., Perenzoni, D., & Mattivi, F. (2014). The influence of storage on the "chemical age" of red wines. *Metabolomics, 10*(5), 816–832. https://doi.org/10.1007/s11306-014-0638-x

Arbulu, M., Sampedro, M. C., Gómez-Caballero, A., Goicolea, M. A., & Barrio, R. J. (2015). Untargeted metabolomic analysis using liquid chromatography quadrupole time-of-flight mass spectrometry for non-volatile profiling of wines. *Analytica Chimica Acta, 858*, 32–41. https://doi.org/10.1016/j.aca.2014.12.028

Baleiras-Couto, M. M., Guedes, R., Duarte, F. L., Fortes, A. M., & Serralheiro, M.-L. (2023). Untargeted metabolomics discriminates grapes and wines from two Syrah vineyards located in the same wine region. *Fermentation, 9*(2), Article 2. https://doi.org/10.3390/fermentation9020145

Cuadros-Inostroza, A., Giavalisco, P., Hummel, J., Eckardt, A., Willmitzer, L., & Peña-Cortés, H. (2010). Discrimination of wine attributes by metabolome analysis. *Analytical Chemistry, 82*(9), 3573–3580. https://doi.org/10.1021/ac902678t

Delcambre, A., & Saucier, C. (2013). High-throughput OEnomics : Shotgun Polyphenomics of wines. *Analytical Chemistry, 85*(20), 9736–9741. https://doi.org/10.1021/ac4021402

Deshaies, S., Cazals, G., Enjalbal, C., Constantin, T., Garcia, F., Mouls, L., & Saucier, C. (2020). Red wine oxidation : Accelerated ageing tests, possible reaction mechanisms and application to Syrah red wines. *Antioxidants, 9*(8). https://doi.org/10.3390/antiox9080663. Article 8.

Dias, A. L. D. S., Fenger, J.-A., Meudec, E., Verbaere, A., Costet, P., Hue, C., … Sommerer, N. (2023). Shades of fine dark chocolate colors : Polyphenol metabolomics and molecular networking to enlighten the Brown from the black. *Metabolites, 13*(5), Article 5. https://doi.org/10.3390/metabo13050667

Echave, J., Barral, M., Fraga-Corral, M., Prieto, M. A., & Simal-Gandara, J. (2021). Bottle aging and storage of wines : A review. *Molecules, 26*(3), Article 3. https://doi.org/10.3390/molecules26030713

Ferreira-Lima, N. E., Burin, V. M., & Bordignon-Luiz, M. T. (2013). Characterization of Goethe white wines : Influence of different storage conditions on the wine evolution during bottle aging. *European Food Research and Technology, 237*(4), 509–520. https://doi.org/10.1007/s00217-013-2019-5

de Freitas, V., & Mateus, N. (2011). Formation of pyranoanthocyanins in red wines : A new and diverse class of anthocyanin derivatives. *Analytical and Bioanalytical Chemistry, 401*(5), 1463–1473. https://doi.org/10.1007/s00216-010-4479-9

Fulcrand, H., Benabdeljalil, C., Rigaud, J., Cheynier, V., & Moutounet, M. (1998). A new class of wine pigments generated by reaction between pyruvic acid and grape anthocyanins. *Phytochemistry, 47*(7), 1401–1407. https://doi.org/10.1016/S0031-9422(97)00772-3

Gambuti, A., Rinaldi, A., Ugliano, M., & Moio, L. (2013). Evolution of phenolic compounds and astringency during aging of red wine : Effect of oxygen exposure before and after bottling. *Journal of Agricultural and Food Chemistry, 61*(8), 1618–1627. https://doi.org/10.1021/jf302822b

García-Guzmán, J. J., Hernández-Artiga, M. P., Palacios-Ponce de León, L., & Bellido-Milla, D. (2015). Selective methods for polyphenols and Sulphur dioxide determination in wines. *Food Chemistry, 182*, 47–54. https://doi.org/10.1016/j.foodchem.2015.02.101

Gil, M., Reynes, C., Cazals, G., Enjalbal, C., Sabatier, R., & Saucier, C. (2020). Discrimination of rosé wines using shotgun metabolomics with a genetic algorithm and MS ion intensity ratios. *Scientific Reports, 10*(1), Article 1. https://doi.org/10.1038/s41598-020-58193-2

Ginjom, I., D'Arcy, B., Caffin, N., & Gidley, M. (2011). Phenolic compound profiles in selected Queensland red wines at all stages of the wine-making process. *Food Chemistry, 125*(3), 823–834. https://doi.org/10.1016/j.foodchem.2010.08.062

Hong, Y.-S. (2011). NMR-based metabolomics in wine science. *Magnetic Resonance in Chemistry, 49*(S1), S13–S21. https://doi.org/10.1002/mrc.2832

Leborgne, C., Lambert, M., Ducasse, M.-A., Meudec, E., Verbaere, A., Sommerer, N., … Cheynier, V. (2022). Elucidating the color of Rosé wines using polyphenol-targeted metabolomics. *Molecules, 27*(4), Article 4. https://doi.org/10.3390/molecules27041359

Leborgne, C., Meudec, E., Sommerer, N., Masson, G., Mouret, J.-R., & Cheynier, V. (2023). Untargeted metabolomics approach using UHPLC-HRMS to unravel the impact of fermentation on color and phenolic composition of Rosé wines. *Molecules, 28*(15), Article 15. https://doi.org/10.3390/molecules28155748

Lopes, P., Richard, T., Saucier, C., Teissedre, P.-L., Monti, J.-P., & Glories, Y. (2007). Anthocyanone A : A Quinone Methide derivative resulting from Malvidin 3-O-glucoside degradation. *Journal of Agricultural and Food Chemistry, 55*(7), 2698–2704. https://doi.org/10.1021/jf062875o

Mateus, N., Silva, A. M. S., Santos-Buelga, C., Rivas-Gonzalo, J. C., & de Freitas, V. (2002). Identification of anthocyanin-Flavanol pigments in red wines by NMR and mass spectrometry. *Journal of Agricultural and Food Chemistry, 50*(7), 2110–2116. https://doi.org/10.1021/jf0111561

Monagas, M., Gómez-Cordovés, C., & Bartolomé, B. (2005). Evolution of polyphenols in red wines from *Vitis vinifera* L. during aging in the bottle. *European Food Research and Technology, 220*(5), 607–614. https://doi.org/10.1007/s00217-004-1108-x

Morehouse, N. J., Clark, T. N., McMann, E. J., van Santen, J. A., Haeckl, F. P. J., Gray, C. A., & Linington, R. G. (2023). Annotation of natural product compound families using molecular networking topology and structural similarity fingerprinting. *Nature Communications, 14*, 308. https://doi.org/10.1038/s41467-022-35734-z

Nikolantonaki, M., Romanet, R., Lucio, M., Schmitt-Kopplin, P., & Gougeon, R. (2022). Sulfonation reactions behind the fate of white wine's shelf-life. *Metabolites, 12*(4), Article 4. https://doi.org/10.3390/metabo12040323

Oliveira, C. M., Ferreira, A. C. S., De Freitas, V., & Silva, A. M. S. (2011). Oxidation mechanisms occurring in wines. *Food Research International, 44*(5), 1115–1126. https://doi.org/10.1016/j.foodres.2011.03.050

Ribéreau-Gayon, P., Glories, Y., Maujean, A., & Dubourdieu, D. (1998). *Traité d'oenologie : Chiie du vin.* Stabilisation et traitement. Dunod.

Rihak, Z., Prusova, B., Kumsta, M., & Baron, M. (2022). Effect of must Hyperoxygenation on sensory expression and chemical composition of the resulting wines. *Molecules, 27*(1), Article 1. https://doi.org/10.3390/molecules27010235

Romanet, R. (2019). *Contribution à l'étude moléculaire de la stabilité oxydative des vins blancs de Bourgogne*. Université Bourgogne France-Comté. https://theses.hal.science/tel-02918125.

Roullier-Gall, C., Hemmler, D., Gonsior, M., Li, Y., Nikolantonaki, M., Aron, A., … Schmitt-Kopplin, P. (2017). Sulfites and the wine metabolome. *Food Chemistry, 237*, 106–113. https://doi.org/10.1016/j.foodchem.2017.05.039

Roullier-Gall, C., Witting, M., Moritz, F., Gil, R. B., Goffette, D., Valade, M., … Gougeon, R. D. (2016). Natural oxygenation of champagne wine during ageing on lees : A metabolomics picture of hormesis. *Food Chemistry, 203*, 207–215. https://doi.org/10.1016/j.foodchem.2016.02.043

Roullier-Gall, C., Witting, M., Tziotis, D., Ruf, A., Gougeon, R. D., & Schmitt-Kopplin, P. (2015). Integrating analytical resolutions in non-targeted wine metabolomics. *Tetrahedron, 71*(20), 2983–2990. https://doi.org/10.1016/j.tet.2015.02.054

Salas, E., Atanasova, V., Poncet-Legrand, C., Meudec, E., Mazauric, J. P., & Cheynier, V. (2004). Demonstration of the occurrence of flavanol–anthocyanin adducts in wine and in model solutions. *Analytica Chimica Acta, 513*(1), 325–332. https://doi.org/10.1016/j.aca.2003.11.084

Schwarz, M., Hofmann, G., & Winterhalter, P. (2004). Investigations on anthocyanins in wines from *Vitis vinifera* cv. Pinotage : Factors influencing the formation of Pinotin A and its correlation with wine age. *Journal of Agricultural and Food Chemistry, 52*(3), 498–504. https://doi.org/10.1021/jf035034f

Tao, Y., García, J. F., & Sun, D.-W. (2014). Advances in wine aging Technologies for Enhancing Wine Quality and Accelerating Wine Aging Process. *Critical Reviews in Food Science and Nutrition, 54*(6), 817–835. https://doi.org/10.1080/10408398.2011.609949

Utpott, M., Rodrigues, E., Rios, A. D. O., Mercali, G. D., & Flôres, S. H. (2022). Metabolomics : An analytical technique for food processing evaluation. *Food Chemistry, 366*, Article 130685. https://doi.org/10.1016/j.foodchem.2021.130685

Vidal, S., Francis, L., Noble, A., Kwiatkowski, M., Cheynier, V., & Waters, E. (2004). Taste and mouth-feel properties of different types of tannin-like polyphenolic compounds and anthocyanins in wine. *Analytica Chimica Acta, 513*(1), 57–65. https://doi.org/10.1016/j.aca.2003.10.017

Vrhovsek, U., Masuero, D., Gasperotti, M., Franceschi, P., Caputi, L., Viola, R., & Mattivi, F. (2012). A versatile targeted metabolomics method for the rapid quantification of multiple classes of Phenolics in fruits and beverages. *Journal of Agricultural and Food Chemistry, 60*(36), 8831–8840. https://doi.org/10.1021/jf2051569

Waterhouse, A., Sacks, G., & Jeffery, D. (2016). *Understanding wine chemistry*. Wiley.

Zhang, X.-K., Lan, Y.-B., Huang, Y., Zhao, X., & Duan, C.-Q. (2021). Targeted metabolomics of anthocyanin derivatives during prolonged wine aging : Evolution, color contribution and aging prediction. *Food Chemistry, 339*, Article 127795. https://doi.org/10.1016/j.foodchem.2020.127795